

### Contents lists available at ScienceDirect

# Giant

journal homepage: www.journals.elsevier.com/giant



# Full-length article

# Highly swellable hydrogels prepared from extensively oxidized lignin

JiHyeon Hwang <sup>a</sup>, Daniella V. Martinez <sup>c,d</sup>, Estevan J. Martinez <sup>c,d</sup>, Gift Metavarayuth <sup>b</sup>, Dustin Goodlett <sup>a</sup>, Qi Wang <sup>b</sup>, Mitra Ganewatta <sup>b,\*</sup>, Michael S. Kent <sup>c,d,\*\*</sup>, Chuanbing Tang <sup>a,\*</sup>

- <sup>a</sup> Department of Chemistry and Biochemistry, University of South Carolina, Columbia, SC 29208, USA
- <sup>b</sup> Ingevity Corporation, 5525 Virginia Avenue, North Charleston, SC 29406, USA
- <sup>c</sup> Joint BioEnergy Institute, Emeryville, CA 94608, USA
- <sup>d</sup> Sandia National Laboratories, Albuquerque, New Mexico, 87185, USA

#### ARTICLE INFO

Keywords: Lignin Polyacid Super absorbent material

### ABSTRACT

Biopolymers such as lignin are gaining renewed appeal due to the need for sustainable materials. Herein, we used chelator-mediated Fenton (CMF) chemistry to oxidize Kraft lignin to develop sustainable super absorbent materials. The CMF chemistry adds oxygen, opens aromatic rings and increases COOH content, producing hydrophilic lignin without depolymerization. UV absorption, molecular weight, elemental analysis, and titration were used to study the chemical compositions of CMF-processed lignin. Then the chemically modified hydrophilic lignin was used to produce lignin-based hydrogels utilizing an aqueous polymerization and cross-linking reaction that enabled tunable properties. The resulting lignin hydrogels absorbed water up to 96% and swelled up to 2400%, as well as being re-swellable in water. These lignin-based hydrogels may be applicable in water-absorbing products in consumer goods and agriculture.

## 1. Introduction

Lignocellulose has been cited as the most abundant and biorenewable natural resource on Earth for manufacturing of sustainable chemicals, polymers and materials [1-4]. The natural polymer, lignin, is a major component of this polymeric mixture and comprises 20-30 wt% of its dry weight [5]. Therefore, much effort has been applied to developing functional materials from lignin, including its use in composite applications [6-8], thermosets [9-11], hydrogels [12,13], to mention just a few. Due to its lower cost, biodegradability, and vast availability, the development of lignin-based materials can help mitigate environmental and economic challenges [14-16]. Lignin is composed mainly of oxygenated phenyl propane monomers, namely guaiacyl (G), syringyl (S), and p-hydroxyphenyl (H) structural units, where the S/G ratio varies with plant type [17-22]. Its poor solubility in water, when the phenolic hydroxyl moieties remain protonated at pH below 10, limits it processability and broad applications [23-25].

To overcome these limitations, a common approach is to cleave ether bonds to depolymerize lignin into a mixture of oligomeric and polymeric fractions, which may undergo additional reactions to yield a broad range of derivatives [26]. The diversity of breakdown products poses a

challenge for generating specific low molecular weight products or intermediates. Another approach is to derive value from the lignin polymer using chemical modifications such as oxidations to increase functionality. In that regard, Fenton-type oxidation procedures have been developed, which lead to a significant increase in hydrophilicity of the natural polymer by increasing hydroxylation of aliphatic and aromatic moieties, and, under more extensive oxidation, opening aromatic rings and generating carboxylic acid groups [27,28]. The effectiveness of Fenton-type oxidized lignin was recently exemplified by Passauer's work with lignin-based hydrogels, where significantly increased swelling capacity was observed when substituting unmodified lignin with Fenton-type oxidized lignin in hydrogel formation [22,27]. In that case mild Fenton oxidation resulted in large increase in carbonyl and phenolic hydroxyl groups, with a small increase in aliphatic OH and carboxyl groups, and only a small degree of aromatic ring opening. Recent work has shown that chelator-mediated Fenton (CMF) reactions can lead to extensive aromatic ring opening, higher carboxylic acid content, and greater water solubility [28]. Introducing more functional groups such as carboxylic acid on lignin makes it versatile for further chemical modification in pursuing valuable end products.

Hydrogels are three-dimensional, hydrophilic polymer networks

https://doi.org/10.1016/j.giant.2022.100106

Received 22 April 2022; Received in revised form 24 May 2022; Accepted 24 May 2022 Available online 26 May 2022

<sup>\*</sup> Corresponding authors.

<sup>\*\*</sup> Corresponding author at: Joint BioEnergy Institute, Emeryville, CA 94608, USA.

E-mail addresses: mitra.ganewatta@ingevity.com (M. Ganewatta), mskent@sandia.gov (M.S. Kent), tang4@mailbox.sc.edu (C. Tang).

capable of holding large amounts of water [29,30]. These properties have enabled the application of hydrogels in many areas, including personal care products, medical applications, batteries and agricultural products for water retention [13,31–34]. Most polymer hydrogels are derived from petroleum chemicals [35], and there is a need for the development of hydrogels from renewable resources [36]. Lignin has been investigated as a class of low-cost renewable polymers for use in water-absorbing value-added materials [37]. However, the fabrication of lignin-based hydrogels usually involves harsh chemical conditions and the use of organic solvents due to the hydrophobicity of lignin, which pose a challenge for large scale production processes. Moreover, little is known about lignin-based hydrogels on water-absorbent properties compared to other commercial superabsorbent hydrogels [38]. Therefore, it is necessary to study lignin-based hydrogels to determine their potential as water-absorbing materials.

Herein, a facile method was developed to produce lignin-based hydrogels in aqueous solutions. We present a strategy that targets theggner generates abundant carboxylic acid groups on CMF modified lignin for imide formation with acrylamide (AAm). When the imide-decorated lignin is subjected to further chemical modification via radical polymerization and crosslinking chemistry, superabsorbent hydrogels can be obtained with tunable properties. The resulting lignin-based hydrogels were analyzed to tailor material properties regarding the swelling ability, extensibility and reprocessability.

#### 2. Results and discussion

### 2.1. Kraft lignin modification via chelator-mediated Fenton reaction

Kraft lignin (Indulin AT, abbreviated as IND) was oxidized using CMF reaction to yield a water-soluble polyacid material (Fig. 1A). This efficient CMF process chemically opens the aromatic rings of lignin and results in an increase in carboxylic acid groups. The process, described in the Methods section, avoids costly separation and concentration steps of a previously-reported CMF process [28]. Attenuated-total reflection infrared (ATR-IR) spectroscopy was used to quantify the aromatic content after CMF reaction. Fig. 1C shows the IR spectra of IND and partially ring-opened lignin (IND-CMF) after the CMF reaction. The aromatic band at 1512 cm<sup>-1</sup> was strongly reduced after the reaction, whereas the bands at 1600 cm<sup>-1</sup> and at 1400 cm<sup>-1</sup> both increased strongly during the reaction and were believed to be due to asymmetric and symmetric C-O carboxylate stretching, respectively [39]. The percentage of aromatic rings remaining after the reaction was estimated from the ratio of the height of the aromatic band at 1512 cm<sup>-1</sup> to either the band at 1600  ${\rm cm}^{-1}$  or the band at 1400  ${\rm cm}^{-1}$  ( $R_{1510/1400~or~1600}$ ). To estimate the percent of aromaticity remaining using IR peak ratios, it is required to have the ratio for the case of 0% aromaticity. We were not able to approach 0% aromaticity using the present method, so the value of the ratio for 0% aromaticity was obtained using a reaction procedure reported previously [28] (Fig. 1B). In that case, the spectrum shows

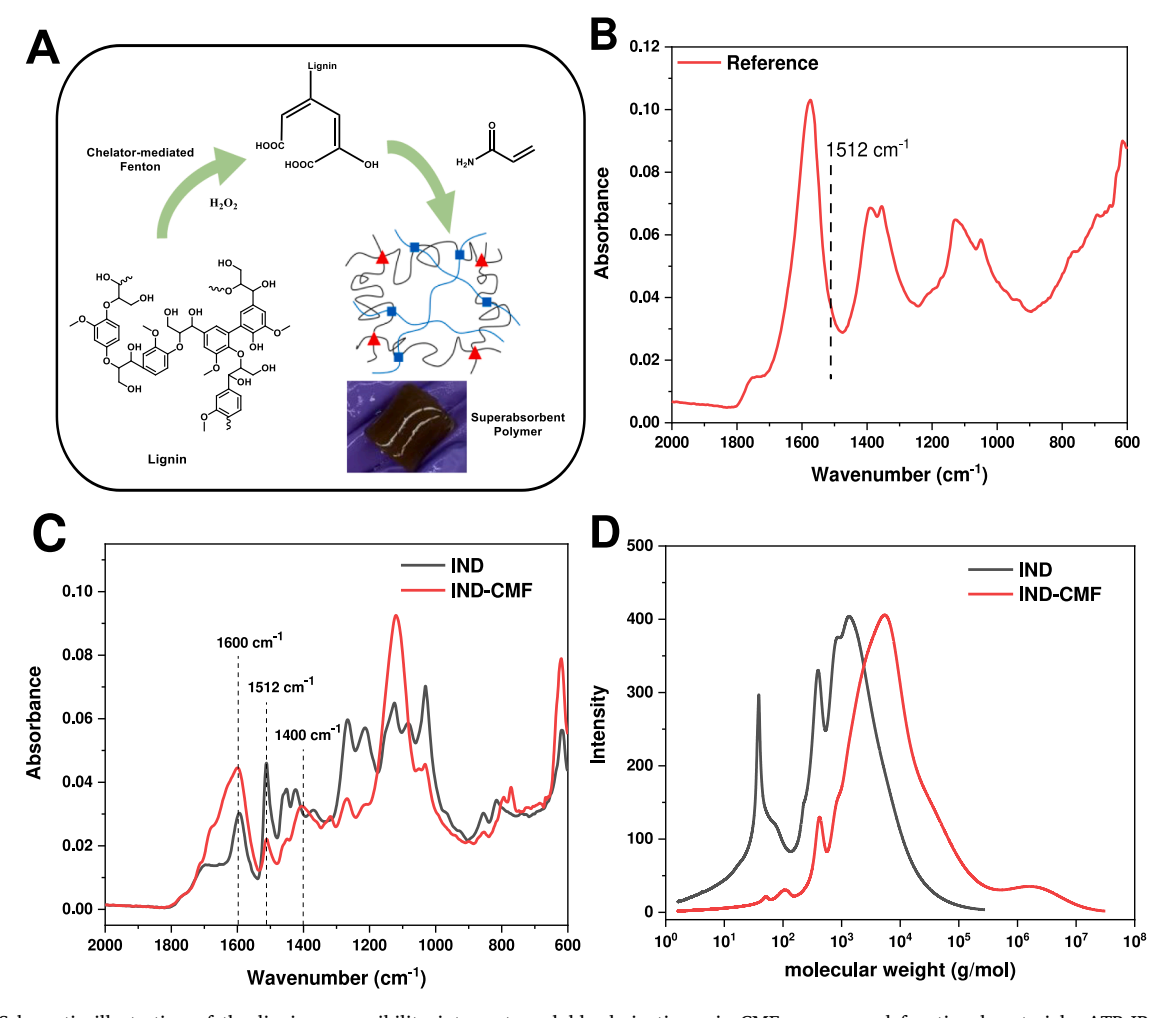


Fig. 1. (A) Schematic illustration of the lignin processibility into water-soluble derivatives via CMF process and functional materials. ATR-IR spectra of (B) Reference measurement for 0% aromaticity and of (C) IND and IND-CMF, and (D) Molecular weight distribution of IND and IND-CMF. Molecular weight distribution was obtained using SEC at pH 11. The peak at low molecular weight for IND is likely due to low molecular weight material generated by the high pH required to solubilize Indulin AT.

complete absence of the aromatic band at  $1512~{\rm cm}^{-1}$ . The following equation (Eq. (1)) waswas used to calculate the aromaticity. The same value for the percentage of aromaticity remaining after reaction (13% aromaticity, Table 1) resulted from using  $1512/1600~{\rm or}~1512/1400$ .

$$Aromaticity (\%) = \frac{\left(R_{1510/1400 \ or \ 1600}\right)_{IND-CMF} - \left(R_{1510/1400 \ or \ 1600}\right)_{reference}}{\left(R_{1510/1400 \ or \ 1600}\right)_{IND} - \left(R_{1510/1400 \ or \ 1600}\right)_{reference}} \times 100$$
(1)

The molecular weight distributions of IND and IND-CMF were characterized by aqueous phase Size Exclusion Chromatography (SEC) with UV detection at 210 nm. Fig. 1D indicates that the CMF conditions used here resulted in a shift of the peak in the distribution to higher molecular weight. This is consistent with prior reports of increased molecular weight for lignosulfonates processed with Fenton reactions under suitable conditions [40,41]. The mobile phase pH 11 was chosen since lignin has better solubility at higher pH, allowing a more accurate molecular weight estimate. The pre- and post-reaction samples shown in Fig. 1D were treated in the same way and so these data demonstrate a significant increase in molecular weight post-reaction. The difference is far outside the small variation that may occur on the timescale of days for lignin samples at pH 11.

Table 2 presents the elemental compositions for IND and IND-CMF, showing that the CMF reaction results in increased oxygen content. Furthermore, titrations were carried out simultaneously for carboxyl group and phenolic hydroxyl group quantification [42]. This method utilizes a combination of aqueous conductometric titration and acid-base titration. A back titration with HCl was carried out after deprotonation of all phenolic hydroxyl and carboxylic acid groups, which occurs upon addition of NaOH to pH > 11.5. Fig. 2 shows the conductometric titration curves in IND and IND-CMF samples. V<sub>1</sub>, V<sub>2</sub>, and V3 correspond to the end of the neutralization of excess NaOH available in the medium, pH 7, and complete protonation of all phenolic hydroxyl and carboxylic acid groups by HCl, respectively. The  $pK_a$  of most carboxylic acids is above 4.5, and the phenolic hydroxyl group in lignin has a p $K_a$  up to 11.5 [43]. Therefore, the titration of phenolic hydroxyl group occurs between V<sub>1</sub> and V<sub>2</sub>, and the carboxyl groups are protonated between V<sub>2</sub> and V<sub>3</sub>. To estimate the phenol and the carboxyl group content, the following equations (Eqs. (2) and (3)) werewe used.

$$Ph - OH\left(\frac{mmol}{g}\right) = (V_2 - V_1) \times \frac{HCl\left(M\right)}{weight\ of\ ash\ free\ lignin} \tag{2}$$

$$COOH\left(\frac{mmol}{g}\right) = (V_3 - V_2) \times \frac{HCl\left(M\right)}{weight\ of\ ash\ free\ lignin} \tag{3}$$

The results are given in Table 2. Lower phenolic hydroxyl group content and higher carboxyl group content were observed in the IND-CMF sample. A higher carboxyl content increases the hydrophilicity of IND-CMF, allowing it to be processed for crosslinking in aqueous solution.

# 2.2. Synthesis and characterization of lignin-based hydrogels

Our objective was to identify a synthetic method to form lignin-based hydrogels with the use of carboxylic acid groups after CMF reaction. We initially employed poly(ethylene glycol) diglycidyl ether (PEGDGE) to crosslink with IND or IND-CMF following the work by Nishida et al.

**Table 1** Absorbance of **IND, IND-CMF**, and **reference** at  $\sim$ 1400 cm $^{-1}$ ,  $\sim$ 1512 cm $^{-1}$ , and  $\sim$ 1600 cm $^{-1}$  from ATR IR spectra.

Peaks (cm <sup>-1</sup> )		Absorbance					
	IND	IND-CMF	Reference (0% aromaticity)				
~1400	0.030	0.032	0.065				
~1512	0.046	0.022	0.036				
~1600	0.030	0.045	0.102				

**Table 2**Chemical compositions of **IND** and **IND-CMF**. (The total percentage is not added up to 100% here, because there are other elements (e.g., sulfur) in ash not tested)

Lignin samples	Elemer	Elemental analysis (%)		Content amount by titration (mmol/g)	
	С	О	Н	СООН	Aromatic OH
IND	61.84	25.54	5.81	1.3	2.76
IND-CMF	48.7	31.80	4.33	1.91	1.4

[44] and Passauer et al. [27]. We expected that IND would be more likely to form a gel than IND-CMF by this method, due to higher phenolic hydroxyl content of IND. However, the gel formed from IND became completely dissolved once immersed in water. Only IND-CMF formed a stable hydrogel but demonstrated weak and brittle properties. The increased amount of COOH groups after the CMF reaction encouraged us to attempt a different chemical modification approach in which we used the COOH groups on IND-CMF for crosslinking.

The carboxylic acid groups on IND-CMF were first targeted for the formation of imide bonds with AAm, followed by the addition of an initiator in which IND-CMF is crosslinked during polymerization (Fig. 3). In the first step (Fig. 3B), AAm forms an imide bond with a carboxylic acid on IND-CMF by using 1-ethyl-3-(3'-dimethylaminopropyl)carbodiimide hydrochloride (EDC·HCl) in 2-(N-morpholino) ethanesulfonic acid (MES buffer). Acidic MES buffer was employed to prevent the regeneration of the carboxyl group via a nucleophilic attack by water on an activated ester. To examine the imidation of IND-CMF with AAm, IND-CMF and AAm with a weight ratio of 1:3 were reacted through EDC in the absence of the crosslinker N,N'-methylenebisacrylamide (MBA), and analyzed by Fourier-transform infrared (FTIR). In the FTIR spectra of AAm-reacted lignin (Fig. 4), a new peak at  $\sim$ 1680 cm<sup>-1</sup> for imide groups appears, and a peak at  $\sim$ 1640 cm<sup>-1</sup>, which is related to carboxyl groups from IND-CMF, decreases. This indicates new bonds formed between -COOH groups of IND-CMF and -NH2 groups of AAm.

In the second step, ammonium persulfate (APS) as an initiator, and N,N,N,N-tetramethylethylenediamine (TEMED) as a crosslinking accelerator, were mixed to prepare covalently crosslinked polyacrylamide (PAAm) with IND-CMF in the presence of the crosslinker MBA. At room temperature, a gel was formed within a few minutes. The main goal of this work is to use lignin as a renewable resource. Therefore, lignin materials should be used as much as possible, but at the same time, they must form a hydrogel. To explore the maximum amount of lignin that can form a hydrogel, lignin-based hydrogels were prepared from different weight ratios of lignin to AAm with various crosslinking densities. The prepared lignin-based hydrogels are referred to as lignin/ PAAm-x:y-z, where x:y is the feed weight ratio between lignin and AAm, and z is the crosslinker (MBA) concentration in mol% with respect to AAm. After the formation of the lignin/PAAm hydrogels, thermal stability studies were conducted. Differential thermogravimetric data (DTG) revealed that the hydrogel (lignin/PAAm-1:3-0.1 as an example) has a two-step degradation profile between 250 and 450 °C, while the sum of IND-CMF and PAAm has three degradation peaks (Fig. 5B). IND-CMF exhibits a two-step degradation at 170-340 °C and 580-740 °C, and PAAm exhibits only one major degradation peak between 310 and 410 °C. The reduced number of degradation peaks from the hydrogel qualitatively supports the gel formation from the two components, IND-CMF and AAm. However, the unmodified IND sample failed to form a hydrogel because of its insolubility in water.

A standard calibration curve of **IND-CMF** at  $\lambda=280$  nm was used to determine the conversion of **IND-CMF** into the hydrogel (Fig. 6). Most of the prepared hydrogels showed nearly 90% conversion of **IND-CMF**, which indicates the high efficiency of reaction in the gel formation. Water swelling properties of lignin/PAAm hydrogels with various crosslinking densities (z=3.9,1.0,0.5, and 0.1) are shown in Fig. 7A. As expected, increasing the amount of crosslinker decreased the swelling.

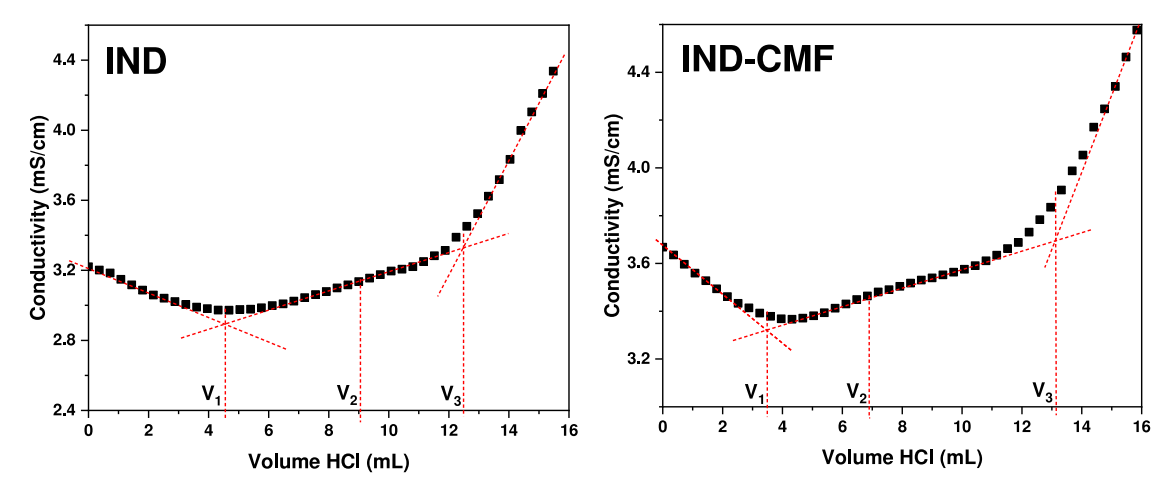


Fig. 2. Conductometric titration curves for IND and IND-CMF lignin samples.

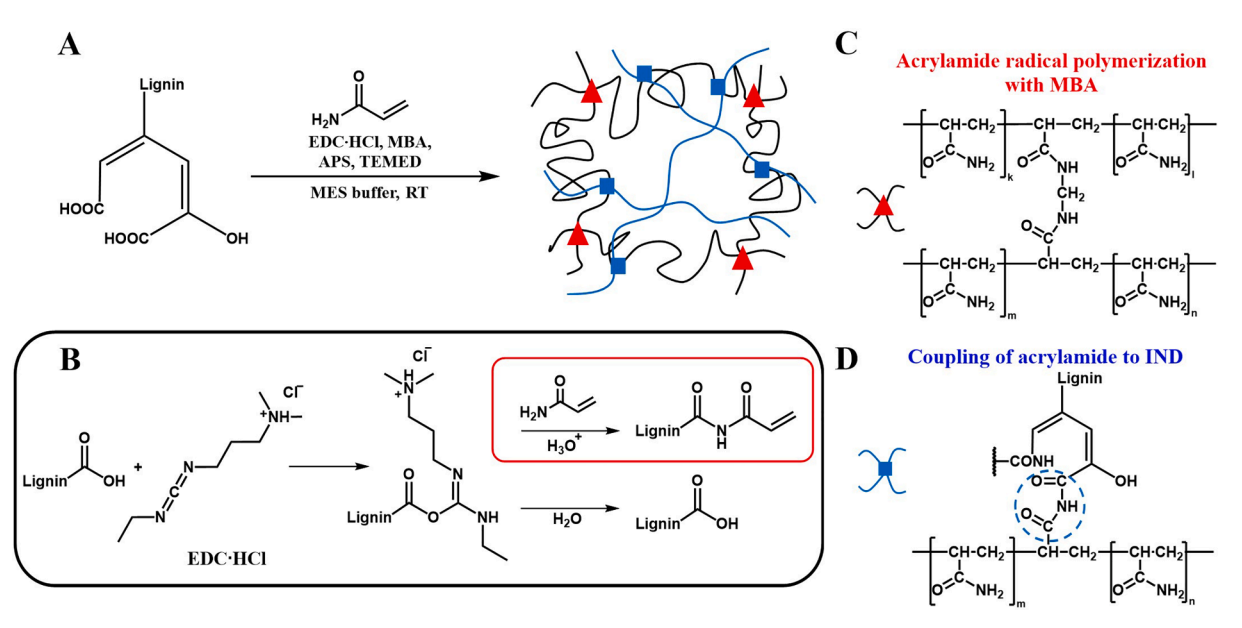


Fig. 3. Preparation of lignin-based hydrogels crosslinked by amino groups on PAAm chains and carboxyl groups on IND-CMF. (A) Overall crosslinking scheme. (B) Imidization of CMF-IND. (C) Polymerization of AAm and crosslinking with MBA. (D) Polymerization of AAm and coupling to imidized IND-CMF.

In particular, lignin/PAAm-1:3-0.1 and lignin/PAAm-1:3-3.9 exhibited swelling ratios at 2400% and 600% (Fig. 7A), respectively. However, decreasing the amount of AAm in the feed ratio from lignin/ PAAm-1:3-0.1 to lignin/PAAm-1:2-0.1 and to lignin/PAAm-1:1-0.1 reduced the degree of crosslinking between -NH2 from AAm and -COOH from IND-CMF, resulting in unstable hydrogels. lignin/PAAm-1:2-0.1, lignin/PAAm-1:1-0.1, lignin/PAAm-1:1-0.5, and lignin/PAAm-1:1-1.0 did not form hydrogels, suggesting the need for higher crosslinking densities. Thus, for these higher lignin/PAAm ratios, a higher crosslinking density improves the gel formation, as observed in lignin/ PAAm-1:2-0.5 and lignin/PAAm-1:1-3.9. All prepared hydrogels exhibited 85 to 96% water uptake (Fig. 7C). As lignin/PAAm-1:3-z was successful in forming hydrogels with all four crosslinker densities, we further examined the porosity of the swollen lignin/PAAm-1:3-z with Scanning Electron Microscope (SEM) (Fig. 8). SEM images reveal that due to less crosslinking of lignin with MBA, lignin/PAAm-1:3-0.1 has a larger average pore size (the average diameter about 1400  $\mu m$ ) than lignin/PAAm-1:3–3.9 (about 500 μm).

To investigate the swelling kinetics of the prepared hydrogels, each gel was immersed in deionized water and swelling was measured at each time interval (Fig. 9). The swelling of the gels increased quickly initially

and then slowed down till it reached equilibrium. In regard to the reusability of hydrogels as water-absorbing products, it is important to characterize the reswelling capability. The swelling and water uptake behaviors of the prepared hydrogels at each consecutive swelling/drying cycle are shown in Fig. 7B and D. In ten swelling/drying cycles, the swelling ratio and the water uptake were nearly constant foreach consecutive cycle. This indicates efficient crosslinking between lignin and PAAm, making the porous structure resilient such that the structure is largely unchanged after several swelling/drying cycles. In all prepared hydrogels, lignin/PAAm-1:3-0.1 exhibited the highest swelling ratio with good reusability. Thus, lignin/PAAm-1:3-z was used in the subsequent studies.

The mechanical properties of **lignin/PAAm-1:3-z** hydrogels cross-linked at various crosslinking densities were examined to explore which composition would lead to gels that are stronger and have greater extensibility. After polymerization, the gel was taken out and glued to two thick papers with  $22.5 \times 7.5 \times 2.3$  mm specimens for tensile tests. All mechanical tests were performed in air, at room temperature. The strain (or stretch ratio),  $\lambda$ , is defined as the ratio of the stretched distance to its initial length. **Lignin/PAAm-1:3-0.1**( $\lambda = 10.5$ ) has much higher strain at break and lower modulus than **lignin/PAAm-1:3-0.5** ( $\lambda = 1.3$ ),

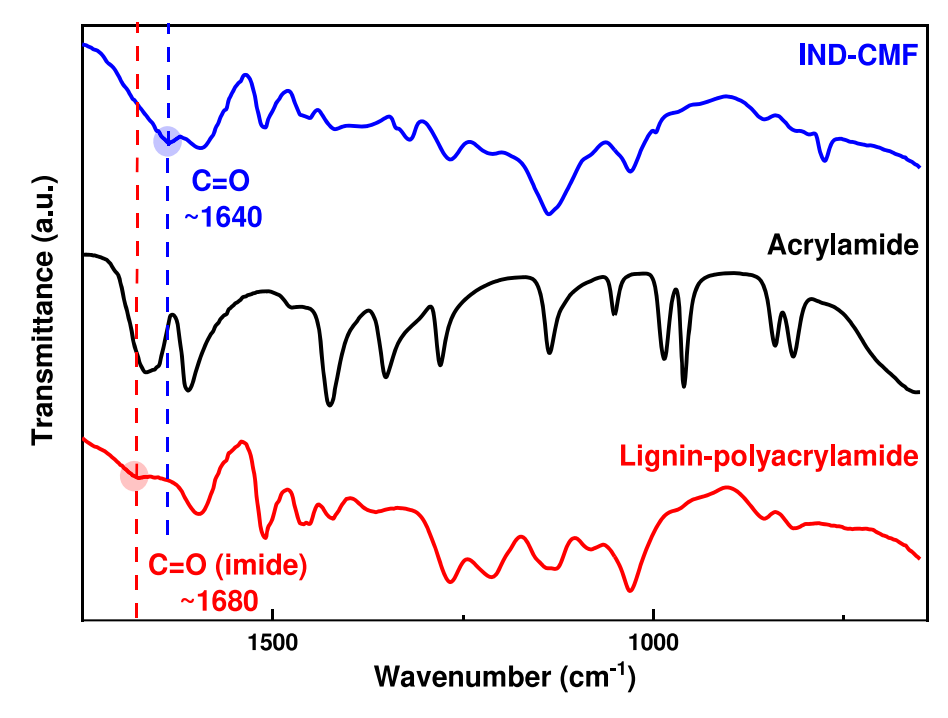


Fig. 4. FTIR spectra of Kraft lignin after CMF reaction (IND-CMF) (blue), AAm (black), and lignin-PAAm in the absence of MBA (red).

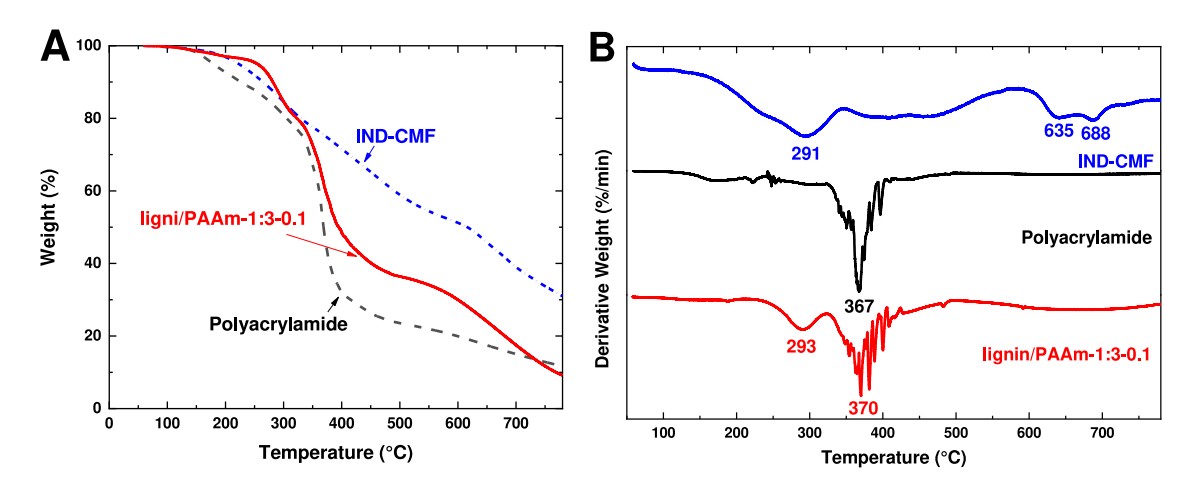


Fig. 5. Thermal degradation profiles of IND-CMF (blue), PAAm (black), and lignin/PAAm-1:3-0.1 hydrogel (red). (A) thermogravimetric analysis (TGA) and (B) differential thermogravimetric (DTG) analysis calculated from TGA data.

**lignin/PAAm-1:3–1.0** ( $\lambda=0.6$ ), and **lignin/PAAm-1:3–3.9** ( $\lambda=0.3$ ) (Fig. 10). The crosslinking density affects the mechanical behavior of the resultant hydrogels. Highly crosslinked hydrogels show higher tensile strength but lower strain at break than the loosely crosslinked hydrogels.

#### 3. Conclusions

In summary, we developed CMF lignin-based hydrogels with tunable properties. We first examined two chemically different lignin samples (IND and IND-CMF) by UV absorption, molecular weight, elemental analysis, and titration to study the chemical compositions. The CMF process provides a simple route to improve the processability of lignin into high-performance materials. This process increased the hydrophilicity and COOH functionality and also increased the molecular weight. To develop functional materials using lignin, we developed a simple aqueous method to synthesize lignin/PAAm hydrogels with tunable properties depending on the crosslink density. The carboxylic groups on IND-CMF were first linked to AAm, and then a hydrogel was formed in

which covalent bonds were formed with PAAm. The resulting lignin hydrogels absorbed water up to 96% and swelled up to 2400%, with good repeatability for cycles of drying and re-swelling in water. Swelling/drying cycles did not degrade their performance even after ten cycles. Depending uponupon desirable properties, the modulus and elongation at break can be tuned by adjusting the gel compositions. The facile processibility and tunability of properties may allow these new materials to be used as superabsorbent products for broad applications.

# 4. Experimental section

### 4.1. General methods and materials

All reagents were used as received unless otherwise stated. Ferric sulfate, 1,2-dihydroxybenzene, poly(ethylene glycol) diglycidyl ether ( $M_n$ =500 g/mol, PEGDGE), acrylamide (AAm), N,N'-methylenebisacrylamide (MBA), and N,N,N,N'-tetramethylethylenediamine (TEMED) were purchased from Sigma-Aldrich. 1-Ethyl-3-(3'-

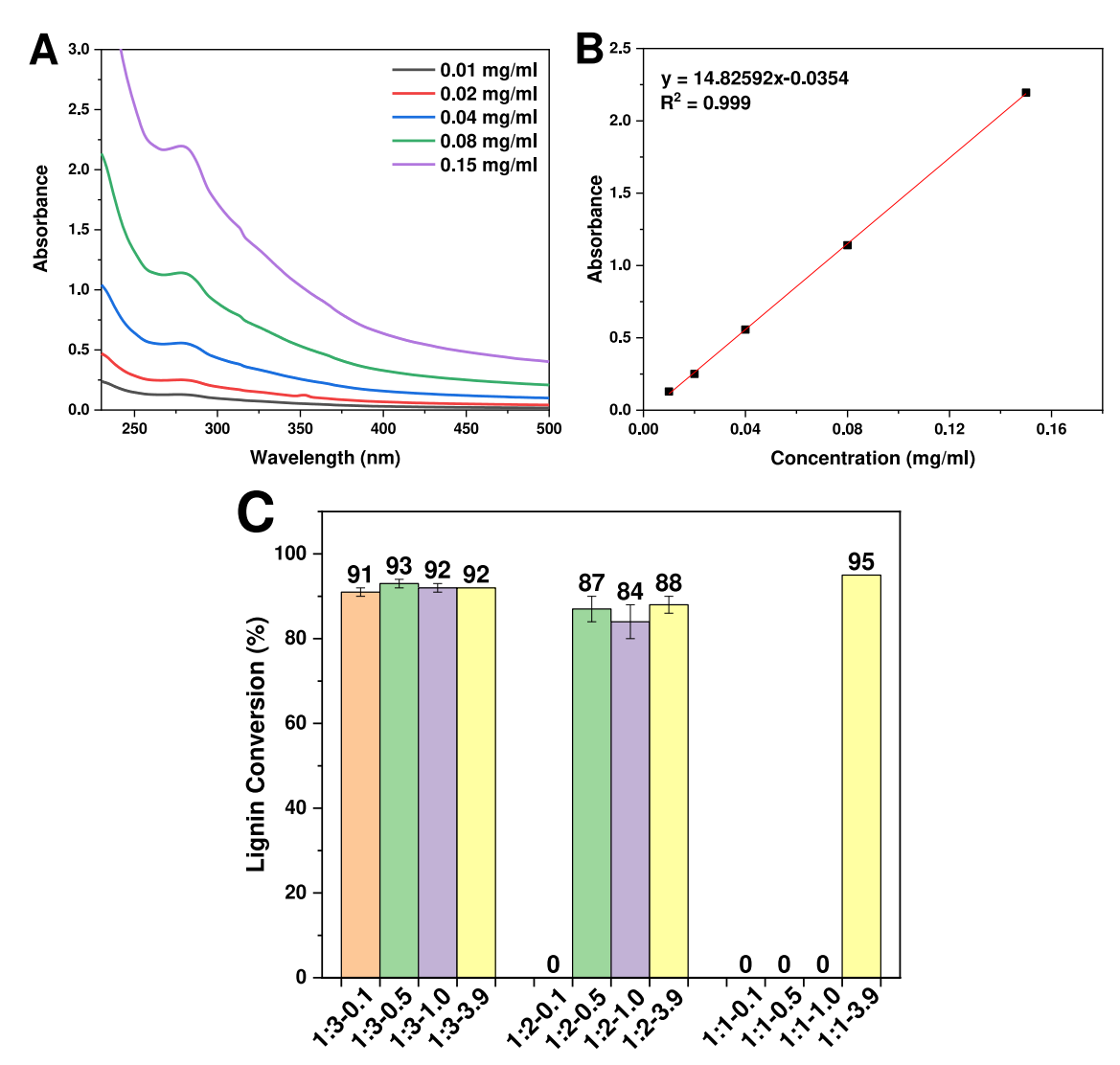


Fig. 6. (A) UV-vis absorption spectra of IND-CMF, (B) Standard calibration curve based on absorption at 280 nm, and (C) Lignin conversion in the final gel (%).

dimethylaminopropyl)carbodiimide hydrochloride (EDC·HCl), ammonium persulfate (APS), and 4-morpholinoethanesulfonic acid hydrate (MES) were purchased from Fisher Scientific. Kraft lignin (Indulin AT) was provided by Ingevity Corporation. All other chemicals were from commercial sources and used as received.

UV-vis spectra were recorded on a SpectraMax M5 Multimode Microplate Reader (Molecular Devices) using water as solvent. Infrared analysis was carried out using solid samples with the aid of a PerkinElmer spectrum 100 FTIR spectrometer. Thermal degradation studies were analyzed with thermogravimetric analysis (TGA) using a TGA Q5000 system. (TA Instruments), ramping from 60 to 800 °C at a heating rate of 10 °C/min under nitrogen atmosphere, and the weight loss was recorded as a function of temperature.

**Chelator-mediated Fenton reaction.** First, 20 g of Indulin AT lignin (IND) (Ingevity), was mixed with 1.35 g ferric sulfate pentahydrate (Acros), 0.40 g 1,2-dihyroxybenzene (Sigma-Aldrich), and 38.25 mL of water. The contents were stirred at room temperature with a magnetic stir bar and the pH was adjusted to 6.0 with 50% sodium hydroxide. To initiate the reaction 8 mL of 35%  $\rm H_2O_2$  (Fisher) was slowly added over a period of 80 min. The pH dropped as the reaction proceeded and was periodically increased to 6.0. The viscosity of the slurry also decreased as the reaction proceeded. Peroxide test strips were used to monitor the progress of the reaction by the decrease in  $\rm H_2O_2$  concentration. When > 90% of the  $\rm H_2O_2$  was consumed, an additional 10 g of IND was added to

the reaction. Then 8 mL of  $35\%~H_2O_2$  was slowly added over a period of 80 min. The pH was again periodically increased to 6.0 and the  $H_2O_2$  concentration was monitored until > 90% consumed. This process of adding 8 mL of  $35\%~H_2O_2$ , periodically adjusting pH to 6.0, and monitoring the  $H_2O_2$  concentration until > 90% consumed was repeated 5 additional times such that the total amount of  $35\%~H_2O_2$  added was 56 mL. When > 90% of the  $H_2O_2$  was consumed after the final addition, the pH was adjusted to 6.0 a final time. Samples (IND-CMF) were taken for analysis by attenuated-total reflection infrared (ATR-IR) and size exclusion chromatography (SEC).

Size Exclusion Chromatography (SEC). Molecular weight distributions were determined using an Agilent 1260 HPLC system with PL Aquagel-PH30 and PL Aquagel-OH 50 columns in series and UV detection at 210 and 270 nm. Samples were diluted to 1∼5 mg/mL by addition of water and the pH was adjusted to 11 by addition of NaOH. The solutions were centrifuged prior to injecting into the HPLC system. The HPLC system contained an in-line filter in front of the analysis column and guard column. The eluent was 1 mM phosphate buffer at pH 9. Polystyrene sulfonate standards (246−280,000 g/mol) were used for calibration. Molecular weights outside this range were obtained by extrapolation. Since pH 11 can cause a chemical change in the material over time, we performed the analysis soon after preparing the samples.

Attenuated Total Reflection Infrared Spectroscopy (ATR-IR). Samples for analysis were prepared by evaporating reaction liquids onto

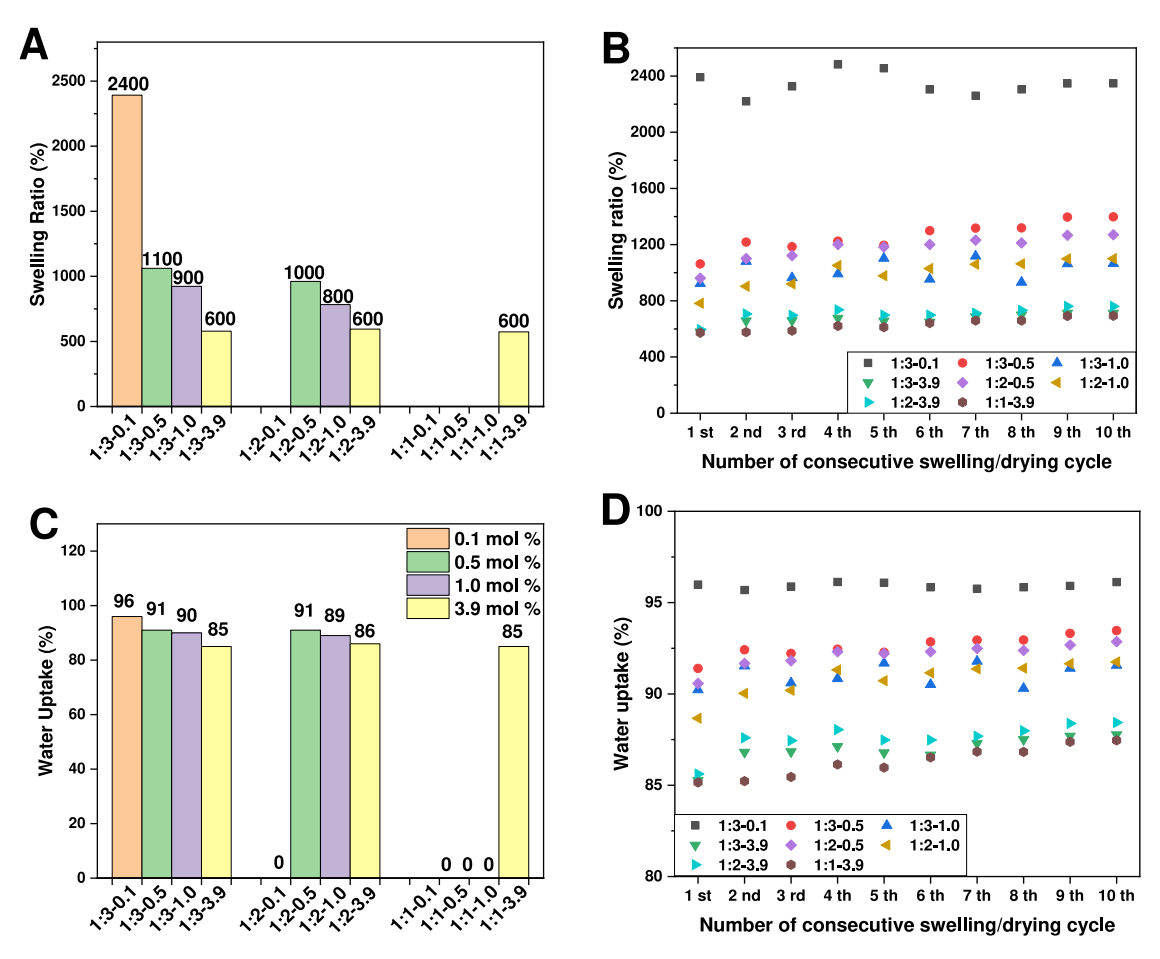


Fig. 7. (A) Swelling ratios and (C) water uptake of lignin/PAAm-x:y-z hydrogels. (B) Swelling capacity and (D) Water uptake of lignin/PAAm-x:y-z hydrogels during consecutive swelling and drying cycles.

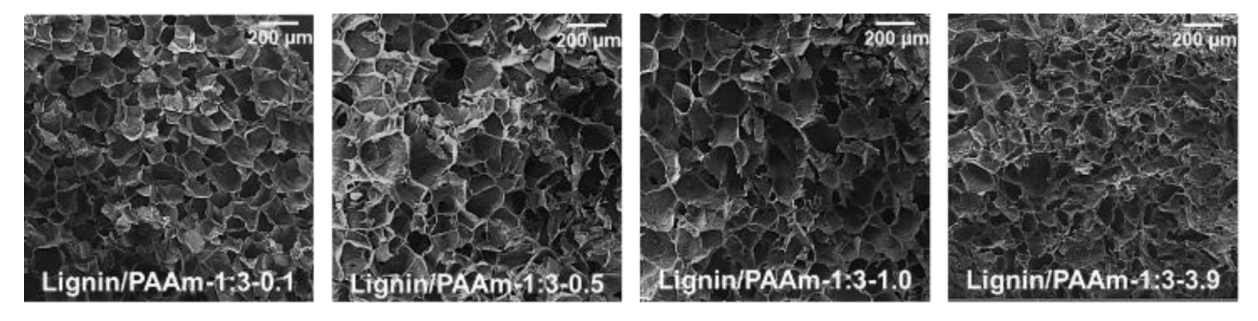


Fig. 8. SEM images of lignin/PAAm-1:3–0.1 (the average diameter of pores:  $\sim 140 \ \mu m$ ), lignin/PAAm-1:3–0.5 ( $\sim 110 \ \mu m$ ), lignin/PAAm-1:3–1.0 ( $\sim 100 \ \mu m$ ), and lignin/PAAm-1:3–3.9 ( $\sim 50 \ \mu m$ ) from left to right, respectively.

Teflon substrates and then drying the films in vacuum. IR spectra were collected with a Bruker LUMOS ATR-FTIR microscope using a germanium probe tip contacting the film. For each sample three spectra were collected and averaged. Each spectrum consisted of 16 averaged scans at a resolution of 4 cm background spectrum collected with no sample present and an atmospheric correction was applied to remove vapor contributions from water and  $\rm CO_2$ .

Phenolic hydroxyl group and carboxyl group determination. Simultaneous conductometric and acidic-base titration by pH was evaluated to provide the phenolic hydroxyl and the carboxyl content amount [42]. 1.0 g of the lignin sample (IND or IND-CMF), 500 mL of deionized water, and 8 mmol of NaOH solution were added and stirred until all dissolved (pH of the mixture was above 11.3). Then, the mixture was titrated with 0.5 M HCl using an auto titrator and the pH was

measured at the same time with a pH meter. The titration rate was 4  $\,$  mL/min of 0.5 M HCl.

**Preparation of lignin hydrogels with PEGDGE.** 150 mg of **IND** or **IND-CMF** was dissolved in 0.3 mL of 3.3 M NaOH aqueous solution and stirred overnight. 0.075 mmol of PEGED was added dropwise to the dissolved lignin mixture and left overnight.

Preparation of lignin/PAAm-x:y-z hydrogels. Using the lignin/PAAm-1:3–0.1 sample as an example, 25 mg of IND-CMF, 75 mg of AAm, 0.2 mg of MBA (0.1 mol% with respect to AAm), and 10.1 mg of EDC·HCl (5 mol% with respect to AAm) were added into 669  $\mu L$  of MES buffer (87 wt%). After stirring for 1 hour at room temperature, 2.4 mg of APS (1.0 mol% with respect to AAm) and 2.1  $\mu l$  of TEMED (1.3 mol% with respect to AAm) were added to the reaction vial under nitrogen atmosphere. The obtained hydrogels were immersed in DI water for a

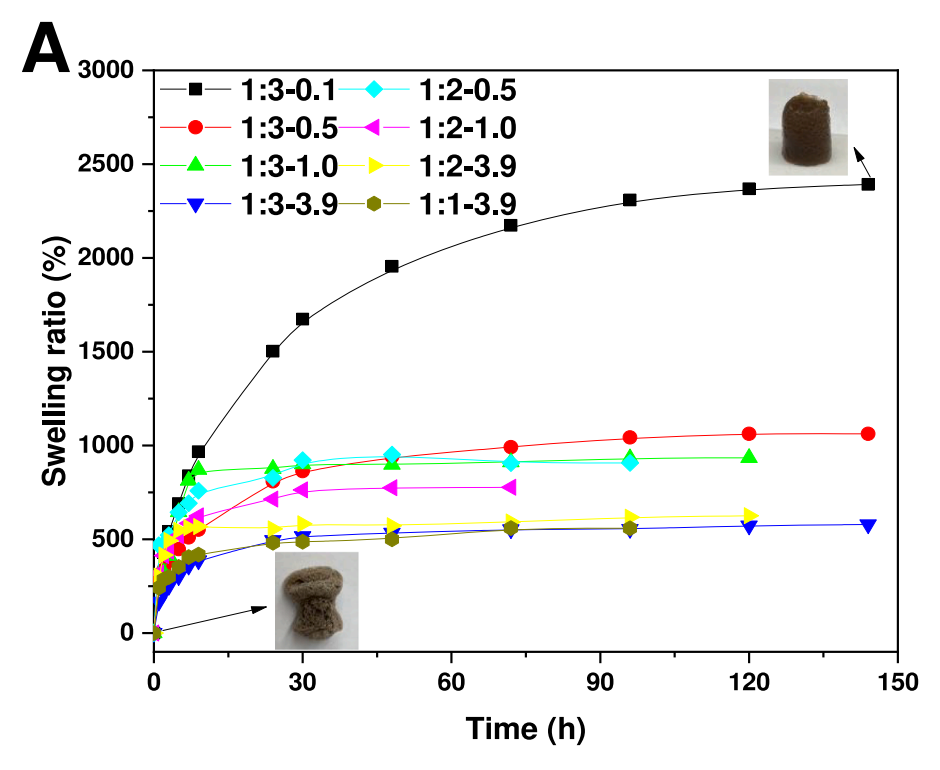


Fig. 9. (A) The swelling kinetics of lignin/PAAm-x:y-z hydrogels at each time interval; inserted photographs from bottom left to top right correspond the freeze dried and hydrated lignin/PAAm-1:3-0.1 hydrogels.

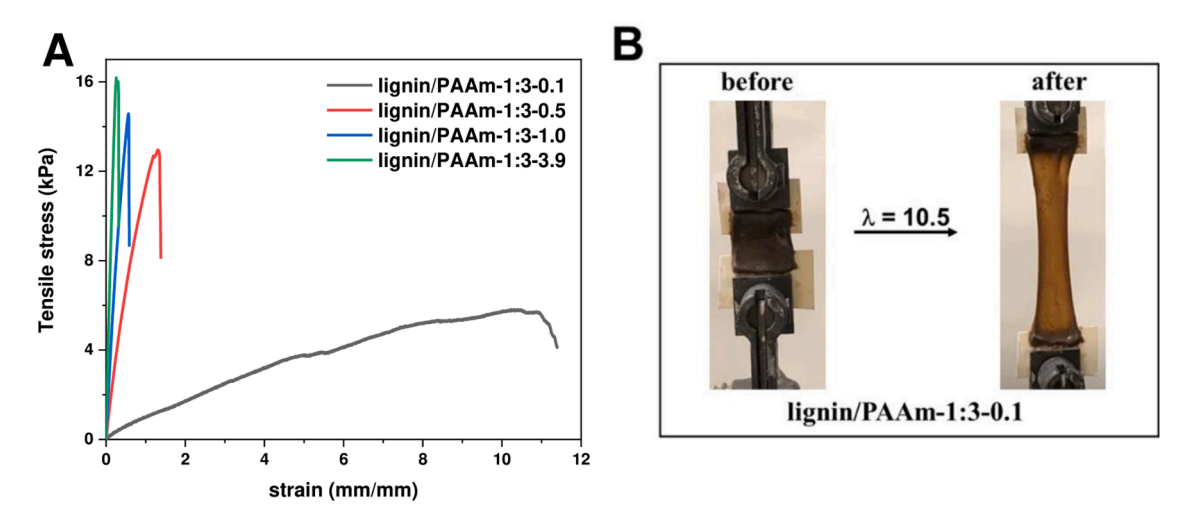


Fig. 10. (A) Stress-strain curves of lignin/PAAm-1:3–0.1, lignin/PAAm-1:3–0.5, lignin/PAAm-1:3–1.0, and lignin/PAAm-1:3–3.9, each stretched to rupture. (B) Photographs of lignin/PAAm-1:3–0.1 hydrogel before and after the gel was stretched to 10.5 times its initial length by a tensile machine.

week to remove unreacted monomers. Fresh water was replaced every day.

Characterization of Lignin/PAAm-x:y-z hydrogels. The compositions of hydrogels were characterized by measuring the UV–vis absorption of IND-CMF at 280 nm. After the gel formation, the prepared gels were immersed in DI water for a week. The water was changed every day with fresh water. Total water solution was collected, then diluted for UV-vis measurement. A standard curve for the water-soluble lignin was established using a series of monomer solution (0.15 mg/mL, 0.08 mg/mL, 0.04 mg/mL, 0.02 mg/mL, and 0.01 mg/mL). The water-soluble lignin conversions (%) in the lignin/PAAm-x:y-z hydrogels were calculated according to the following equation (Eq. (4)).

Conversion (%) = 
$$\frac{m_0 - c_t \times V}{m_0} \times 100$$
 (4)

where  $m_0$  indicates the initial amount of **IND-CMF**, V is the volume of the diluted solution, and  $c_t$  is the concentration of the diluted solution, which was obtained from the UV-vis absorption spectra.

**Swelling Studies.** Hydrogels were dried fully after washing. The dried gels were measured with the initial mass and were then immersed in deionized water until they reached equilibrium. The water content (%) of hydrogels was assessed by comparing weight of the swollen sample  $(m_w)$  and dried sample  $(m_d)$  and calculated according to the following equation (Eq. (5)).

water content (%) = 
$$\frac{m_w - m_d}{m_w} \times 100$$
 (5)

The swelling ratio (%) of hydrogels was calculated according to the following equation (Eq. (6)).

swelling ratio (%) = 
$$\frac{m_w - m_d}{m_d} \times 100$$
 (6)

**Scanning Electron Microscopy (SEM).** The samples were dried using a freeze dryer, then coated with gold using Denton Desk II sputter Coater for 60 s and observed by Tescan Vega-3 SBU SEM.

Consecutive Swelling and Drying Cycle. The prepared hydrogels were initially freeze dried. When the gels were completely dried, the weight of the samples were recorded. Then the samples were soaked in DI water. When they reached equilibrium, the weights of the swollen samples were recorded. The swelling and drying cycle was repeated a total of 10 times.

**Mechanical Test.** Tensile tests were carried out with an Instron 5543A. The <code>lignin/PAAm-x:y-z</code> hydrogels were freshly prepared in a mold ( $25 \times 25$  mm) before test. The prepared gels were taken out from the mold and glued to two thick papers with specimens of  $23 \times 7.5 \times 2.3$  mm for the mechanical test. A crosshead speed of testing was 7.5 mm/min.

#### **Declaration of Competing Interest**

We declare there are no conflicts of interest or competing financial interests.

### Acknowledgements

This work is supported by U.S. Department of Energy Bioenergy Technologies Office under Award Number DE-EE0008912 and partially by U.S. National Science Foundation (DMR-1806792 to C.T.). Sandia National Laboratories is a multimission laboratory managed and operated by National Technology & Engineering Solutions of Sandia, LLC, a wholly owned subsidiary of Honeywell International Inc., for the U.S. Department of Energy's National Nuclear Security Administration under contract DE-NA0003525.

#### Supplementary materials

Supplementary material associated with this article can be found, in the online version, at doi:10.1016/j.giant.2022.100106.

### References

- C.H. Zhou, X. Xia, C.X. Lin, D.S. Tong, J. Beltramini, Catalytic conversion of lignocellulosic biomass to fine chemicals and fuels, Chem. Soc. Rev. 40 (11) (2011)
- [2] F.H. Isikgor, C.R. Becer, Lignocellulosic biomass: a sustainable platform for the production of bio-based chemicals and polymers, Polym. Chem. 6 (25) (2015) 4497–4559.
- [3] Z. Wang, M.S. Ganewatta, C. Tang, Sustainable polymers from biomass: bridging chemistry with materials and processing, Prog. Polym. Sci. 101 (2020), 101197.
- [4] M.S. Ganewatta, Z. Wang, C. Tang, Chemical syntheses of bioinspired and biomimetic polymers toward biobased materials, Nat. Rev. Chem. 5 (11) (2021) 753–772.
- [5] A. Tolbert, H. Akinosho, R. Khunsupat, A.K. Naskar, A.J. Ragauskas, Characterization and analysis of the molecular weight of lignin for biorefining studies, Biofuels Bioprod. Biorefin. 8 (6) (2014) 836–856.
- [6] H.M. Wang, T.Q. Yuan, G.Y. Song, R.C. Sun, Advanced and versatile lignin-derived biodegradable composite film materials toward a sustainable world, Green Chem. 23 (11) (2021) 3790–3817.
- [7] M. Cho, F.K. Ko, S. Renneckar, Molecular orientation and organization of technical lignin-based composite nanofibers and films, Biomacromolecules 20 (12) (2019) 4485–4493.
- [8] Y. Xu, L. Yuan, Z. Wang, P.A. Wilbon, C. Wang, F. Chu, C. Tang, Lignin and soy oil-derived polymeric biocomposites by "grafting from" RAFT polymerization, Green Chem. 18 (18) (2016) 4974–4981.
- [9] L. Yuan, Y. Zhang, Z. Wang, Y. Han, C. Tang, Plant oil and lignin-derived elastomers via thermal azide-alkyne cycloaddition click chemistry, ACS Sustain. Chem. Eng. 7 (2) (2019) 2593–2601.

[10] C. Gioia, G. Lo Re, M. Lawoko, L. Berglund, Tunable thermosetting epoxies based on fractionated and well-characterized lignins, J. Am. Chem. Soc. 140 (11) (2018) 4054–4061.

- [11] M.E. Jawerth, C.J. Brett, C.d. Terrier, P.T. Larsson, M. Lawoko, S.V. Roth, S. Lundmark, M. Johansson, Mechanical and morphological properties of ligninbased thermosets, ACS Appl. Polym. Mater. 2 (2) (2020) 668–676.
- [12] D.-f. Zheng, L. Hu, X.Q. Qiu, Recent advances in lignin-based hydrogels and its synthesis and applications, lignin utilization strategies: from processing to applications, ACS Symp. Ser. (2021) 207–229.
- [13] Y. Guo, J. Bae, Z. Fang, P. Li, F. Zhao, G. Yu, Hydrogels and hydrogel-derived materials for energy and water sustainability, Chem. Rev. 120 (15) (2020) 7642–7707.
- [14] A.J. Ragauskas, G.T. Beckham, M.J. Biddy, R. Chandra, F. Chen, M.F. Davis, B. H. Davison, R.A. Dixon, P. Gilna, M. Keller, Lignin valorization: improving lignin processing in the biorefinery, Science 344 (6185) (2014), 1246843.
- [15] M.E. Himmel, S.Y. Ding, D.K. Johnson, W.S. Adney, M.R. Nimlos, J.W. Brady, T. D. Foust, Biomass recalcitrance: engineering plants and enzymes for biofuels production, Science 315 (5813) (2007) 804–807.
- [16] M.S. Ganewatta, H.N. Lokupitiya, C. Tang, Lignin biopolymers in the age of controlled polymerization, Polymers 11 (7) (2019) 1176 (Basel).
- [17] M. Alherech, S. Omolabake, C.M. Holland, G.E. Klinger, E.L. Hegg, S.S. Stahl, From lignin to valuable aromatic chemicals: lignin depolymerization and monomer separation via centrifugal partition chromatography, ACS Cent. Sci. 7 (11) (2021) 1831–1837.
- [18] W. Lan, M.T. Amiri, C.M. Hunston, J.S. Luterbacher, Protection group effects during α,γ-diol lignin stabilization promote high-selectivity monomer production, Angew. Chem. Int. Ed. 57 (5) (2018) 1356–1360.
- [19] W. Lan, J.B. DeBueren, J.S. Luterbacher, Highly selective oxidation and depolymerization of  $\alpha,\gamma$ -diol-protected lignin, Angew. Chem. Int. Ed. 58 (9) (2019) 2649–2654.
- [20] L. Shuai, M.T. Amiri, Y.M. Questell-Santiago, F. Héroguel, Y. Li, H. Kim, R. Meilan, C. Chapple, J. Ralph, J.S. Luterbacher, Formaldehyde stabilization facilitates lignin monomer production during biomass depolymerization, Science 354 (6310) (2016) 329–333.
- [21] W.M. Goldmann, J. Ahola, O. Mankinen, A.M. Kantola, S. Komulainen, V.V. Telkki, J. Tanskanen, Determination of phenolic hydroxyl groups in technical lignins by ionization difference ultraviolet spectrophotometry (Δε-IDUS method), Period. Polytech. Chem. Eng. (2016).
- [22] L. Passauer, Highly swellable lignin hydrogels: novel materials with interesting properties, functional materials from renewable sources, ACS Symp. Ser. (2012) 211–228.
- [23] H. Lange, S. Decina, C. Crestini, Oxidative upgrade of lignin-recent routes reviewed, Eur. Polym. J. 49 (6) (2013) 1151–1173.
- [24] Z. Sun, B. Fridrich, A. De Santi, S. Elangovan, K. Barta, Bright side of lignin depolymerization: toward new platform chemicals, Chem. Rev. 118 (2) (2018) 614–679.
- [25] N. Zhou, W. Thilakarathna, Q. He, H. Rupasinghe, A review: depolymerization of lignin to generate high-value bio-products: opportunities, challenges, and prospects, Front, Front. Energy Res. 9 (2022), 758744.
- [26] C. Crestini, H. Lange, M. Sette, D.S. Argyropoulos, On the structure of softwood Kraft lignin, Green Chem. 19 (17) (2017) 4104–4121.
- [27] L.F. Lars Passauer, F. Liebner, Activation of pine Kraft lignin by Fenton-type oxidation for cross-linking with oligo(oxyethylene) diglycidyl ether, Wood Res. Technol. 65 (3) (2011) 319–326.
- [28] M.S. Kent, J. Zeng, N. Rader, I.C. Avina, C.T. Simoes, C.K. Brenden, M.L. Busse, J. Watt, N.H. Giron, T.M. Alam, M.D. Allendorf, B.A. Simmons, N.S. Bell, K.L. Sale, Efficient conversion of lignin into a water-soluble polymer by a chelator-mediated Fenton reaction: optimization of H2O2use and performance as a dispersant, Green Chem. 20 (13) (2018) 3024–3037.
- [29] E.M. Ahmed, Hydrogel: preparation, characterization, and applications: a review, J. Adv. Res. 6 (2) (2015) 105–121.
- [30] F. Ullah, M.B.H. Othman, F. Javed, Z. Ahmad, H.M. Akil, Classification, processing and application of hydrogels: a review, Mater. Sci. Eng. C 57 (2015) 414–433.
- [31] A.S. Hoffman, Hydrogels for biomedical applications, Adv. Drug Deliv. Rev. 64 (2012) 18–23.
- [32] Y. Qiu, K. Park, Environment-sensitive hydrogels for drug delivery, Adv. Drug Deliv. Rev. 53 (3) (2001) 321–339.
- [33] M.R. Guilherme, F.A. Aouada, A.R. Fajardo, A.F. Martins, A.T. Paulino, M.F. Davi, A.F. Rubira, E.C. Muniz, Superabsorbent hydrogels based on polysaccharides for application in agriculture as soil conditioner and nutrient carrier: a review, Eur. Polym. J. 72 (2015) 365–385.
- [34] H. Li, P. Yang, P. Pageni, C. Tang, Recent advances in metal-containing polymer hydrogels, Macromol. Rapid Commun. 38 (14) (2017), 1700109.
- [35] J.R. Banu, S. Kavitha, R.Y. Kannah, T.P. Devi, M. Gunasekaran, S.H. Kim, G. Kumar, A review on biopolymer production via lignin valorization, Bioresour. Technol. 290 (2019), 121790.
- [36] D.A. Baker, T.G. Rials, Recent advances in low-cost carbon fiber manufacture from lignin, J. Appl. Polym. Sci. 130 (2) (2013) 713–728.
- [37] V.K. Thakur, M.K. Thakur, Recent advances in green hydrogels from lignin: a review, Int. J. Biol. Macromol. 72 (2015) 834–847.
- [38] N. Mazloom, R. Khorassani, G.H. Zohury, H. Emami, J. Whalen, Lignin-based hydrogel alleviates drought stress in maize, Environ. Exp. Bot. 175 (2020), 104055.
- [39] J.J. Max, C. Chapados, Infrared spectroscopy of aqueous carboxylic acids: malic acid, J. Phys. Chem. A 106 (27) (2002) 6452–6461.
- [40] D.V. Martinez, A. Rodriguez, M.A. Juarros, E.J. Martinez, T.M. Alam, B. A. Simmons, K.L. Sale, S.W. Singer, M.S. Kent, Depolymerization of lignin for

- biological conversion through sulfonation and a chelator-mediated Fenton reaction, Green Chem.  $24\ (4)\ (2022)\ 1627-1643$ .
- [41] D. Areskogh, G. Henriksson, Chemical Pulping: fenton's reaction: a simple and versatile method to structurally modify commercial lignosulphonates, Nord. Pulp. Pap. Res. J. 26 (1) (2011) 90–98.
- [42] L. Serrano, E.S. Esakkimuthu, N. Marlin, M.C. Brochier-Salon, G. Mortha, F. Bertaud, Fast, easy, and economical quantification of lignin phenolic hydroxyl
- groups: comparison with classical techniques, Energy Fuels 32 (5) (2018) 5969–5977.
- [43] D.L. Woerner, J.L. McCarthy, Lignin. 24. Ultrafiltration and light-scattering evidence for association of Kraft lignins in aqueous solutions, Macromolecules 21 (7) (1988) 2160–2166.
- [44] M. Nishida, Y. Uraki, Y. Sano, Lignin gel with unique swelling property, Bioresour. Technol. 88 (1) (2003) 81–83.